Gain and carrier temperature response of semiconductor laser media to short optical pulses

T. V. Sarkisyan and A. T. Rosenberger

Department of Physics and Center for Laser and Photonics Research, Oklahoma State University, Stillwater, Oklahoma 74078

A. N. Oraevsky

Lebedev Physical Institute, Russian Academy of Sciences, Leninsky Prospect 53, Moscow 117924, Russia

D. K. Bandy

Department of Physics and Center for Laser and Photonics Research, Oklahoma State University, Stillwater, Oklahoma 74078

Received August 26, 1999; revised manuscript received February 1, 2000

The gain and carrier temperature response of semiconductor laser media to picosecond optical pulses with various pulse energies is obtained by means of a model that is based on rate equations extended to include the carrier energy density equation. The temperature dynamics are obtained from the carrier energy density by use of a quasi-equilibrium Fermi–Dirac distribution. We study the cases of media whose prepulse states are strongly absorbing, transparent, and strongly amplifying at the frequency of the pulse. The results show that the various physical processes that influence the gain and carrier temperature contribute differently, depending on both the initial state of the medium and the pulse energy. In particular, the influence of free-carrier absorption and two-photon absorption on the dynamics of the carrier temperature and the gain coefficient is discussed in detail. © 2000 Optical Society of America [S0740-3224(00)01305-9]

OCIS codes: 320.0320, 320.5390, 320.7130, 250.5980, 190.5970, 190.4720, 140.5960.

1. INTRODUCTION

During the past decade semiconductor gain dynamics on ultrashort time scales have become an important area of research. Interest in this subject has been fueled by experiments that study the response of semiconductor laser amplifiers to ultrashort (picosecond and shorter) optical pulses. In particular, these experiments[1–5] show gain nonlinearity, i.e., suppression and recovery of the gain of the order of a picosecond. This type of gain response is believed to be a result of the peculiar behavior of the carrier ensemble on short time scales, specifically, that of dynamic carrier heating; this belief is supported by theoretical calculations.[6–16]

Although the carrier heating influence on gain dynamics has attracted much attention, the dynamic behavior of the carrier temperature is usually not a target of research. In most cases carrier temperature appears only as part of an *ad hoc* explanation of the nonlinear behavior of the gain. However, the efficiency of carrier heating by an external signal depends on the gain; furthermore, changes in the gain influence the carrier temperature. This feedback leads to interesting dynamic behavior of both the gain and the carrier temperature.

Note that carrier temperature dynamics are not the only way to describe carrier heating and its influence on gain in semiconductor laser diodes and other optoelectronic devices. In fact, the carrier temperature is often left out of the dynamic picture. This is the case when very short pulses (those less than 0.1–0.2 ps) are considered. These femtosecond pulses create non equilibrium carrier ensembles, in which the carrier temperature is not a meaningful physical parameter. Therefore it is reasonable to choose the microscopic description[17–22] over a combination of rate and energy balance equations.[15,16]

The above arguments suggest the following limits for using the carrier temperature as a dynamic variable in a description of the gain dynamics on a short time scale: (i) The time scale should be long enough for the quasi-equilibrium approximation to be reasonable (longer than ~0.1 ps); (ii) the approach based on carrier temperature dynamics should offer significant simplicity, in both the solution of the problem and the interpretation of results, as compared with the microscopic approach. With these limits the carrier temperature is a useful parameter in the description of the dynamics of semiconductor diode laser, amplifiers, and passive systems, and it deserves special attention from the points of view of both physics and applications.

In this paper the behavior of both the carrier temperature and the gain function, under the influence of external optical pulses with different energies is discussed. We focus on the differences in the dynamic response of absorbing, transparent, and amplifying media. Our theory is based on modified rate equations, including an equation for carrier energy density.[15,16] The paper is organized as follows. The model equations and the gain func-

tion are described in Section 2, while the relations among dynamic variables are discussed in Section 3. Section 4 presents the results of calculations and corresponding analysis. The results are summarized in Section 5.

2. MODIFIED RATE EQUATIONS

The dynamics of a semiconductor laser medium and its response to an external pulse can be described by rate equations for photon density, N_p, carrier density, N, and carrier energy density, U:

$$\frac{dN_p}{dt} = -\frac{1}{\tau_p}N_p + \Gamma\nu_{gr}gN_p + \Gamma\beta_{sp}\frac{N}{\tau_s} - \nu_{gr}s_{FCA}NN_p - \nu_{gr}s_{TPA}N_p^2 + \kappa N_{px}, \tag{1a}$$

$$\frac{dN}{dt} = J - \frac{N}{\tau_e} - \nu_{gr}gN_p + \nu_{gr}s_{TPA}N_p^2, \tag{1b}$$

$$\frac{dU}{dt} = Q - \frac{U}{\tau_s} - \frac{U - U_1}{\tau_1} - \hbar\omega\nu_{gr}gN_p + \hbar\omega\nu_{gr}s_{FCA}NN_p + 2\hbar\omega\nu_{gr}s_{TPA}N_p^2, \tag{1c}$$

where τ_p is the photon lifetime, Γ is the confinement factor, ν_{gr} is the group velocity, β_{sp} is the spontaneous emission factor, τ_s is the spontaneous lifetime of carriers, s_{FCA} is the free-carrier absorption (FCA) cross section, s_{TPA} is the two-photon absorption (TPA) cross section, N_{px} is the external pulse photon density, κ is the coupling coefficient, and g is the gain function (in cm^{-1}). J is the effective carrier injection rate, given by $J = \eta_{inj}I/q_eV$, where η_{inj} is the efficiency of carrier injection, I is the bias current, q_e is the elementary charge, and V is the active region volume. In Eq. (1b), τ_s is the carrier recombination time, which is equal to the spontaneous lifetime of carriers τ_s if we ignore nonradiative recombination processes and Auger recombination. Note that in Eqs. (1a) and (1b) it is assumed that the densities of electrons and holes are equal; they are denoted by N. In Eq. (1c), Q represents the pumping term. In general, it is an independent external factor. However, in some cases it is possible to express this term explicitly through the carrier and lattice temperatures, the injection current, or, in the case of optical pumping, the energy of the pumping pulse (see Section 3). The second term in Eq. (1c) represents carrier energy loss that is due to spontaneous recombination. This term is written in analogy with the spontaneous radiative recombination term in the carrier density equation. The third term accounts for the energy density relaxation that is due to interaction with the lattice. This term is assumed to be exponential with a characteristic time τ_l determined by carrier–lattice interactions. The parameter U_l is the carrier energy density at the temperature of the lattice [see Eq. (13) below]. The last three terms represent the major heating (or cooling) factors, namely, interband transitions, FCA, and TPA; $\hbar\omega$ is the photon energy.

Equations (1) differ from the widely used rate equations for semiconductor lasers[23–26] by virtue of the additional equation for the carrier energy density and the terms that account for TPA and FCA. The main function that links Eqs. (1) is the gain function. The free-carrier quasi-equilibrium theory in the two-band approximation leads to the following expression for the gain function:[26]

$$g = C_0(\omega, T_l)|M|^2\rho_r[f(\mu_e, T_e) + f(\mu_h, T_h) - 1] = g(\omega, T_l, T_e, T_h, \mu_e, \mu_h). \tag{2}$$

where C_0 is a function that depends on the material parameters and the transition frequency, M is the transition matrix element, ρ_r is the reduced density of states, f is the Fermi distribution function, and $\mu_{e(h)}$ and $T_{e(h)}$ are the electron (hole) chemical potential and temperature, respectively.

Thus the gain is a function of the transition frequency, the chemical potentials, and the temperatures of the electron and hole ensembles. The material parameters are functions of the lattice temperature T_l. Therefore the gain function depends on the lattice temperature as well. Nevertheless, because of the higher heat capacity of the lattice as compared with that of the carrier ensembles, the lattice temperature changes more slowly than the carrier temperatures, and for sufficiently fast processes one can assume that T_l is a constant.

The carrier temperatures appear in the gain function through the electron and hole distribution functions:

$$f(\varepsilon_e, \mu_e, T_e) - \frac{1}{2} + f(\varepsilon_h, \mu_h, T_h) - \frac{1}{2} = \frac{1}{2}\left[\tanh\left(\frac{\mu_e - \varepsilon_e}{2k_BT_e}\right) + \tanh\left(\frac{\mu_h - \varepsilon_h}{2k_BT_h}\right)\right], \tag{3}$$

where k_B is the Boltzmann constant. Choosing the top of the valence band to be the zero level of energy, one can write

$$\varepsilon_e = \varepsilon_g + (\hbar\omega - \varepsilon_g)\bar{m}/m_e, \tag{4a}$$

$$-\varepsilon_h = (\hbar\omega - \varepsilon_g)\bar{m}/m_h, \tag{4b}$$

where $\bar{m} = m_em_h/(m_e + m_h)$, $m_{e(h)}$ is the electron (hole) effective mass, and ε_g is the bandgap energy. These relations lead to

$$\varepsilon_e = \varepsilon_g - (m_h/m_e)\varepsilon_h. \tag{5}$$

At zero temperature the highest energy that the carriers can have is equal to their chemical potential:

$$\mu_e = \varepsilon_g - (m_h/m_e)\mu_h. \tag{6}$$

For nonzero temperatures, Eq. (6) is not exact but remains a good approximation even at room temperature. Using the above relations, we can write the right-hand side of Eq. (3) as

$$\frac{1}{2}\left\{\tanh\left(\frac{\mu_e - \varepsilon_e}{2k_BT_e}\right) + \tanh\left[\left(\frac{m_e}{m_h}\right)\frac{\mu_e - \varepsilon_e}{2k_BT_h}\right]\right\}. \tag{7}$$

Note here that the argument of the second hyperbolic tangent is much smaller than that of the first because of the small electron–hole effective mass ratio (provided that the hole temperature is not much lower than the electron temperature, which is usually the case because the carrier ensembles interact with each other more effectively than with the lattice). This indicates that the gain function has a much weaker dependence on hole temperature

variations than on electron temperature variations. As a result, the second term on the right-hand side of Eq. (3) can be neglected:

$$f(\varepsilon_e, \mu_e, T_e) + f(\varepsilon_h, \mu_h, T_h) - 1 \cong \frac{1}{2}\tanh\left(\frac{\mu_e - \varepsilon_e}{2k_B T_e}\right), \tag{8}$$

and one can also take the hole temperature to be equal to the electron temperature. Therefore, from this point on, it is sufficient to consider only the electron dynamics, and we drop the subscript index e.

Using the previous argument, we can write the gain function [Eq. (2)] in a simple form:

$$g = G(\omega)\tanh\left(\frac{\mu - \varepsilon}{2k_B T}\right), \tag{9}$$

where $G(\omega)$ is a function that needs to be specified for each particular case.

In our calculations we use the approach used by Rivlin and colleagues,[27,28] which approximates the electron density of states near the band edge as an exponential. Then, with the same considerations that lead to relation (8), the reduced density of states is well approximated by the electron density of states; therefore the gain function has the form of Eq. (9), with

$$G(\omega) = \frac{n_{gr}\hbar\pi^2 c^2}{\tau_s \omega^2 n^3}\rho_0 \exp\left(\frac{\hbar\omega}{\varepsilon_t}\right), \tag{10}$$

for transitions from the band edge, including tail states. Here n is the index of refraction, n_{gr} is the group refractive index, and $\rho_0 \equiv (\xi/\varepsilon_t)\exp(-\varepsilon_g/\varepsilon_t)$, where ξ is the density of dopants and ε_t is an empirical band tail parameter. In heterostructure lasers, where the active region is not necessarily doped, the parameter ξ can also be considered an empirical parameter. The material parameters (refractive index, bandgap, etc.) may also depend on the lattice temperature or frequency. Although Eq. (10) is derived for homostructure lasers, it represents the temperature and frequency dependence of the gain function for heterostructure lasers very well. Figure 1 demonstrates the behavior of the gain [Eqs. (9) and (10)] in GaAs as a function of the photon energy for fixed temperature or chemical potential. When used in calculations of the dynamical behavior of semiconductor laser media, the gain function [Eq. (9)] intrinsically accounts for gain nonlinearity that is due to carrier heating because it reflects the carrier temperature dependence of the gain.

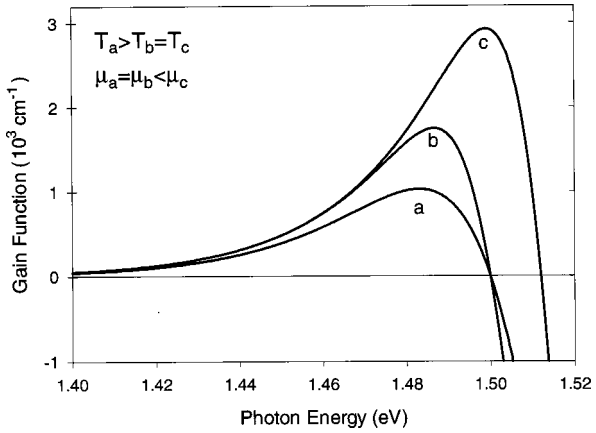

Fig. 1. Gain [Eq. (9)] as a function of photon energy for fixed temperature or chemical potential. Equation (10) is used for $G(\omega)$. Curves a and b correspond to different temperatures ($T_a > T_b$), and curves b and c correspond to different chemical potentials ($\mu_b < \mu_c$).

The chemical potential is related to the carrier density through the integral

$$N(\mu, T) = \int \rho(\varepsilon) f(\varepsilon, \mu, T)\mathrm{d}\varepsilon, \tag{11}$$

where ρ is the density of states and ε is the carrier energy. For a given temperature, this relationship between the carrier density and the chemical potential allows us to describe the behavior of the chemical potential by using the carrier density equation (1b). However, the carrier temperatures are changing under the influence of external factors. The equations necessary to describe these changes can be obtained through energy balance among the carrier ensemble, the lattice, and the photons. The energy density of the carrier ensemble is defined by the integral

$$U(\mu, T) = \int \rho(\varepsilon) f(\varepsilon, \mu, T)\varepsilon\mathrm{d}\varepsilon. \tag{12}$$

Using this expression, we can specify the expression for U_l:

$$U_l = \int \rho(\varepsilon) f(\varepsilon, \mu(T_l), T_l)\varepsilon\mathrm{d}\varepsilon. \tag{13}$$

Equations (1), along with the expression for the gain function [Eq. (9)], constitute a closed set of equations. The dynamic variables N and U are related to μ and T through integrals (11) and (12). For analysis of the dynamics, these relationships among variables must be derived for each particular case. The calculation of integrals (11) and (12), in general, does not lead to analytical expressions. The numerical solution of Eqs. (1), (9), (11), and (12) is a complicated problem. Therefore analytical expressions relating N, U, μ, and T are desirable because they significantly simplify the analysis.

3. RELATIONS AMONG DYNAMIC VARIABLES

In this section we consider for the medium a simple model that allows us to obtain the desired analytical expressions and to describe carrier temperature dynamics in semiconductor laser media (e.g., gain suppression due to carrier heating in semiconductor amplifiers[15,16]).

Integrals (11) and (12) can be simplified with the assumptions that are used to obtain Eqs. (9) and (10) and with the following approximation for the Fermi–Dirac function[15,16]:

$$f(\varepsilon, \mu, T) = \begin{cases} 1 - 0.5\exp[(\varepsilon - \mu)/k_B T] & \varepsilon \leqslant \mu \\ 0.5\exp[(\mu - \varepsilon)/k_B T] & \varepsilon > \mu \end{cases}. \tag{14}$$

This approximation is more accurate for lower temperatures and is exact at 0 K. The resulting expressions for the electron ensemble are[15,16]

$$N(\mu,\theta) = \frac{\rho_0 \varepsilon_t}{1 - \theta^2} \exp\left(\frac{\mu}{\varepsilon_t}\right), \tag{15}$$

$$U(\mu,\theta) = N\left[\mu + \varepsilon_t \frac{(3\theta^2 - 1)}{1 - \theta^2}\right], \tag{16}$$

where we introduce the dimensionless temperature $\theta = k_B T/\varepsilon_t$.

The pumping term in the energy density equation (1c) represents an effective energy flow that is due to carrier injection into the active region. It can be expressed explicitly through other dynamic variables by use of the following logic: Q is related to the pumping term J in the carrier density equation (1b) as U is related to N, i.e., through an expression similar to Eq. (16):

$$Q = J\left[\tilde{\mu} + \varepsilon_t \frac{(3\theta_l^2 - 1)}{1 - \theta_l^2}\right], \tag{17}$$

where $\theta_l = k_B T_l/\varepsilon_t$. Because the injected carriers interact with the lattice before reaching the active region, their temperature is the same as the lattice temperature; $\tilde{\mu}$ is determined as follows: Noting that the effective injection rate can also be presented as the loss rate of carriers from the adjacent region to the active region, we write $J = \tilde{N}/\tau_s$, where $\tilde{N}$ is the carrier density in the adjacent region. Now we use Eq. (15) to determine $\tilde{\mu}$:

$$\tilde{\mu} = \varepsilon_t \ln\left[\tilde{N} \frac{(1 - \theta_l^2)}{\rho_0 \varepsilon_t}\right]. \tag{18}$$

Substituting Eq. (18) in Eq. (17), we obtain

$$Q = J\varepsilon_t \left\{\ln\left[J\tau_s \frac{(1 - \theta_l^2)}{\rho_0 \varepsilon_t}\right] - \frac{1 - 3\theta_l^2}{1 - \theta_l^2}\right\}. \tag{19}$$

The analytical expressions presented above are accurate for low temperatures, $T < \varepsilon_t/k_B$. For a band tail parameter, $\varepsilon_t \sim 20$ meV, they are accurate for temperatures as high as ~230 K. For higher temperatures, the integral expressions (11) and (12) should be used instead of the analytical approximations (15) and (16). Our analysis of gain and temperature dynamics, presented in Section 4, is based on solving Eqs. (1) with Eqs. (9), (10), and (19). The carrier temperature and chemical potential in Eq. (9) are found from Eqs. (15) and (16).

4. GAIN AND CARRIER TEMPERATURE DYNAMICS

The model without TPA, described in Sections 2 and 3, is used to investigate the gain and carrier temperature dynamics in semiconductor laser media.[15,16] The investigation results in a straightforward physical description of the gain behavior observed in pump–probe experiments near the transparency region, particularly those of Ref. 3. In this paper we focus on the response of the gain and carrier temperature to an external pulse, using material parameters relevant to GaAs.[29]

We choose for our investigation a 1-μm-thin sample that is assumed to be antireflection coated so that the medium is a single-pass system. For such a short sample (of length L), one can use the photon density equation (1) with $\tau_p = L/\nu_{gr}$; for longer samples, the photon density equation should be replaced by a traveling-wave equation (see, e.g., Ref. 30). In our analysis we are interested in dynamics related to carrier heating effects, i.e., local carrier temperature deviation from the lattice temperature. The spatial behavior of the carrier temperature is irrelevant here, since the external pulse front always confronts a carrier ensemble unperturbed by the pulse itself. In addition, the carrier ensemble is not influenced by carriers from adjacent regions already heated by the pulse because the pulse travels much faster than the heat transfers. Thus, unless the pump–probe experiment is numerically simulated or pulse reshaping is considered, the short samples (those short enough to exclude propagation effects such as pulse reshaping) are convenient for the investigation of carrier temperature and gain coefficient dynamics because the analysis is not complicated by spatial effects.

The calculations are performed for a lattice temperature $T_l = 70$ K. The choice of low lattice temperature allows us to use the analytical expressions (15)–(19), which simplify the problem to ordinary differential equations. For high lattice temperatures, as was mentioned at the end of Section 3, the equations are integrodifferential, and a simple analysis is no longer possible. However, the qualitative picture that is obtained from this simple analysis can correctly describe the room-temperature behavior as well. This is evident from the comparison of the earlier results based on this model[16] and on the experiments reported in Refs. 1–5, most of which are carried out at room temperature. Indeed, the character of interactions that we are considering is similar for liquid nitrogen and room temperatures; only the numerical values of some parameters are different.

The bandgap narrowing due to many-body effects is accounted for by consideration of the bandgap energy as a function of carrier density according to the expression[31]

$$\varepsilon_g(N) = \varepsilon_g - 1.6 \times 10^{-8} N^{1/3}, \tag{20}$$

where $\varepsilon_g = 1.5077$ eV.

We use the following parameter values: photon energy $\hbar\omega = 1.5$ eV, spontaneous recombination time $\tau_s = 10^{-9}$ s, energy density relaxation time $\tau_l = 5 \times 10^{-13}$ s, band tail parameter $\varepsilon_t = 20$ meV, dopant concentration $\xi = 10^{18}\,\mathrm{cm}^{-3}$, refractive index $n = 3.319$, group-velocity index $n_{gr} = 4.0$, spontaneous emission factor $\beta_{sp} = 10^{-5}$, and confinement factor $\Gamma = 0.3$. The external pulse is coupled to the system by the coupling coefficient κ; because our sample is antireflection coated, $\kappa = 1/\tau_p$.

The FCA cross section is chosen to be $s_{FCA} = 5 \times 10^{-18}\,\mathrm{cm}^2$; this value leads to 10 cm^{-1} FCA losses for $N = 2 \times 10^{18}\,\mathrm{cm}^{-3}$, which is consistent with the values given in the literature.[32] The TPA cross section can be obtained from $s_{TPA} \equiv \beta_2 \nu_{gr} \hbar\omega$, where β_2 is the TPA coefficient, which is calculated with the expression found in Ref. 33:

$$\beta_2 = K\frac{\sqrt{E_p}}{n^2\varepsilon_g{}^3}\left(2\frac{\hbar\omega}{\varepsilon_g}-1\right)^{3/2}\left(\frac{\hbar\omega}{\varepsilon_g}\right)^{-5}. \tag{21}$$

Here E_p is a nearly material-independent constant equal to 21 eV and K is a material-independent constant equal to 1940 in units such that β_2 is measured in centimeters per gigawatts. For given parameter values and ε_g calculated according to Eq. (20), we obtain $\beta_2 \sim 6.28$ cm/GW. This is a considerable underestimation as compared with experimental results.[33,34] To have more realistic values for our calculations we use Eq. (21) with $K = 9700$, which gives $\beta_2 \sim 31.4$ cm/GW. These values are given only for orientation, because β_2 is not a constant owing to dependence on ε_g, which is a dynamic variable. Nevertheless, note that the value of β_2 does not change significantly when the change in carrier density is within a couple of orders of magnitude.

We choose the lattice temperature as the initial condition for the carrier temperature in each numerical experiment. The steady-state values of all the dynamic variables before the arrival of the external pulse are determined by the carrier injection rate. By the proper choice of the injection one can make the sample absorbing, transparent, or amplifying. It is convenient to use, as a reference, the injection rate J_0, which makes the sample transparent without any external signal. From Eq. (1b) we find the relationship between J_0 and the carrier density at transparency to be $J_0 = N_{\mathrm{tr}}/\tau_e$, and, because in our model N_{tr} is a dynamic variable, the value of J_0 depends on system parameters and is determined numerically. In particular, for the parameters given above, $N_{\mathrm{tr}} \cong 1.67 \times 10^{18}\,\mathrm{cm}^{-3}$.

The transparency condition here is identified formally with the condition of zero gain. However, because the FCA and the TPA are not included in the gain function, the sample appears to be transparent in response to the external optical signal only when there is a small amplification in the medium that compensates for the FCA, the TPA, and other minor losses. In other words, the sample must be slightly amplifying to exhibit zero net absorption, i.e., for the sample to return to its prepulse state immediately after the departure of the external pulse. In addition, because the transparency is achieved by compensation of FCA and TPA (as well as of interband absorption), which are dependent on the photon density, the external pulse energy and duration determine whether the sample will appear transparent.

The behavior of the amplifying medium is extensively studied both experimentally and theoretically[1–16] by means of diode laser amplifiers. Carrier dynamics in an absorbing medium are investigated by use of saturable absorbers (reverse-biased p-i-n structures).[35–37] In this study we focus on carrier temperature and gain dynamics in a forward-biased p-n structure for various carrier injection rates. We change the external pulse energy and monitor the state of the medium before and after the pulse as well as the gain and carrier temperature dynamics during the interaction. We use optical pulses with a Gaussian profile:

$$N_{\mathrm{px}}(t) = \frac{W}{\sqrt{\pi}\Delta\tau}\exp\left[-\left(\frac{t}{\Delta\tau}\right)^2\right], \tag{22}$$

where $\Delta\tau = \Delta\tau_{\mathrm{FWHM}}/2\sqrt{\ln 2}$. The value of W is determined through the pulse energy, which is calculated with

$$\mathscr{E} = c \cdot \hbar\omega\int\int\int N_{\mathrm{px}}(x, y, t)\,\mathrm{d}x\,\mathrm{d}y\,\mathrm{d}t, \tag{23}$$

where x and y are transverse coordinates. We assume that the external pulse cross section is larger than the transverse area of the active region so that the sample responds to an almost constant intensity profile. Therefore the energy injected into the sample by the external signal is

$$\mathscr{E}_x = W\hbar\omega sc, \tag{24}$$

where s is the transverse area of the active region, which is assumed to be completely covered by the central part of the external pulse. Typical values for the transverse area of the active region are approximately 10^{-8}–$10^{-9}\,\mathrm{cm}^2$ (Ref. 24).

Generally, depending on carrier injection rate and pulse energy, we observe the following short-time behavior of the gain: (i) gain suppression in an amplifying medium; (ii) absorption enhancement both in a transparent medium and in an absorbing medium close to transparency; and (iii) absorption suppression in an absorbing medium far from transparency. The calculations show that in all these cases the suppression or enhancement is caused by substantial carrier heating and relaxes on the time scale of τ_l. Our model is able to predict this variety of behavior by use of an approximate analytical expres-

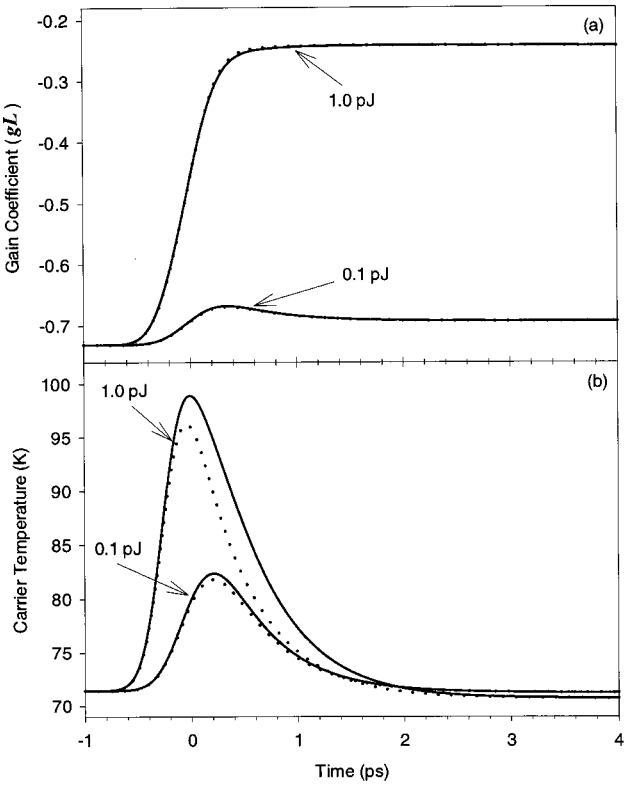

Fig. 2. Behavior of (a) the dimensionless gain coefficient and of (b) the carrier temperature, influenced by 0.1- and 1.0-pJ pulses with (solid curve) and without (dotted curve) FCA and TPA in an initially absorbing ($g < 0$) medium.

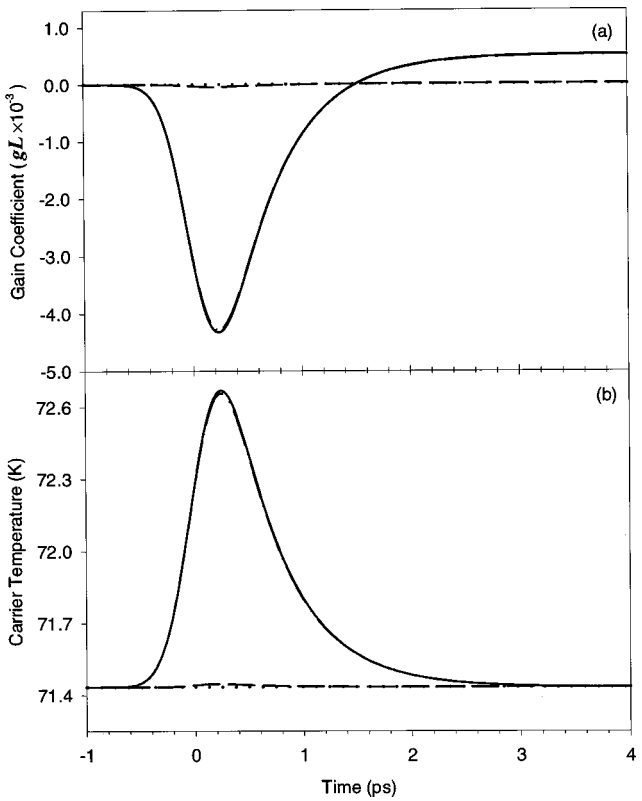

Fig. 3. Behavior of (a) the dimensionless gain coefficient and of (b) the carrier temperature, influenced by a 0.1-pJ pulse with FCA and TPA (solid curve), without FCA (dashed curve), without TPA (dashed–dotted curve), and without both (dotted curve) in an initially transparent ($g = 0$) medium.

sion for the gain function (see details in Ref. 16). All the behavior described above is consistent with experimental observations.[1–5]

All the calculations described in this paper are performed with 0.5-ps (FWHM) pulses. For a fixed carrier injection rate, we change the external pulse energy and observe the dynamics. Then we choose another value for the carrier injection rate and repeat the calculations. The results presented in this paper are obtained by means of pulse energies $\mathscr{E}_x = 0.1, 1.0, 5.0, 25.0$ pJ with injection rates $J_e = 0.4J_0$ (absorbing medium: $g < 0$), $J_e = 1.0J_0$ (transparent medium: $g = 0$), and $J_e = 1.6J_0$ (amplifying medium: $g > 0$). Note that $\mathscr{E}_x$ is not the total energy of the external pulse but the energy of the portion of the pulse that overlaps the cross section of the active region of the sample. The parameters are chosen in such a way that during the calculations the values of all the dynamic variables remain within the limits of validity of the analytical expressions (15) and (16).

In Figs. 2(a)–5(a) below we demonstrate the behavior of the dimensionless gain coefficient (gL) influenced by pulses with energies $\mathscr{E}_x = 0.1, 1.0$ pJ. The corresponding carrier temperature behavior is presented in Figs. 2(b)–5(b) below. For comparison, we also include the graphs obtained without including FCA and TPA (dotted curves in all the figures). For the transparent sample (Figs. 3 and 4 below), we include graphs that are obtained by including either FCA or TPA only. Note that all the figures show that the carrier temperature is higher than the lattice temperature even when the external signal is absent. This is a result of so-called recombination heating: increase in carrier temperature in a recombining degenerate Fermi ensemble.[38–40]

The case of an initially absorbing medium is shown in Fig. 2. Absorption suppression (the gain coefficient peak) caused by carrier heating is noticeable for the 0.1–pJ pulse [the lower curves in Fig. 2(a)] and not for the 1.0-pJ pulse (the upper curves), although in both cases there is substantial carrier heating, as shown in Fig. 2(b). The carrier temperature behavior is quite similar for both pulse energies; it is interesting that the 0.1-pJ pulse heats the carriers almost as effectively as the 1.0-pJ pulse. To understand this behavior we compare the carrier densities before ($t = -4$ ps) and after ($t = +5$ ps) the external pulse. The carrier density changes from $\sim 0.668 \times 10^{18}\,\mathrm{cm}^{-3}$ to $\sim 0.763 \times 10^{18}\,\mathrm{cm}^{-3}$ for the 0.1-pJ pulse and to $\sim 1.38 \times 10^{18}\,\mathrm{cm}^{-3}$ for the 1.0-pJ pulse. The 1.0-pJ pulse pumps more energy into the medium and produces a greater increase in the carrier density. However, this increase in carrier density tends to lower the carrier temperature because absorption involves cold carriers. As a result, we see ~2.5 times difference in peak carrier temperature changes (~12 and ~30 K) for pulses with energies that differ by a factor of 10. The dotted curves in Fig. 2 represent the results of calculations without FCA and TPA. Note that in both cases the influence

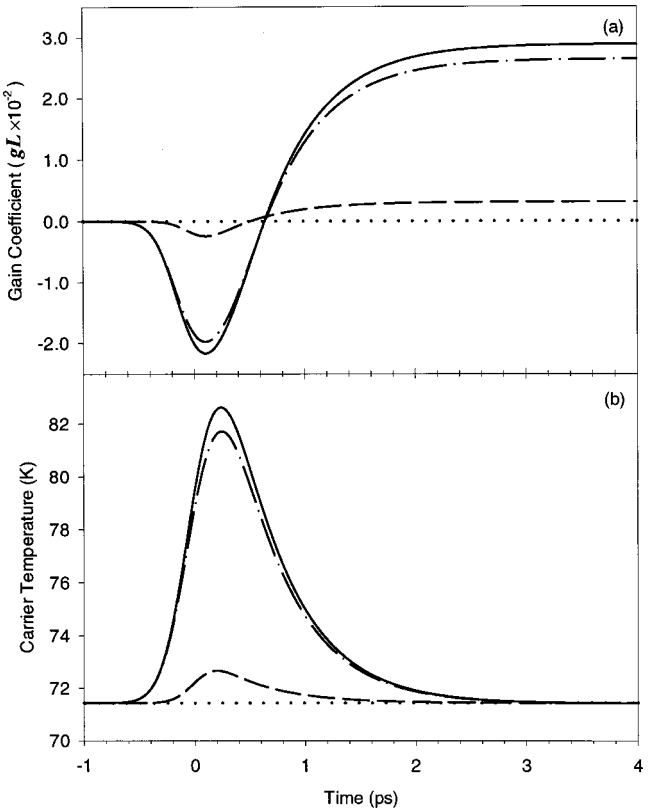

Fig. 4. Behavior of (a) the dimensionless gain coefficient and of (b) the carrier temperature, influenced by a 1-pJ pulse with FCA and TPA (solid curve), without FCA (dashed curve), without TPA (dashed–dotted curve), and without both (dotted curve) in an initially transparent ($g = 0$) medium.

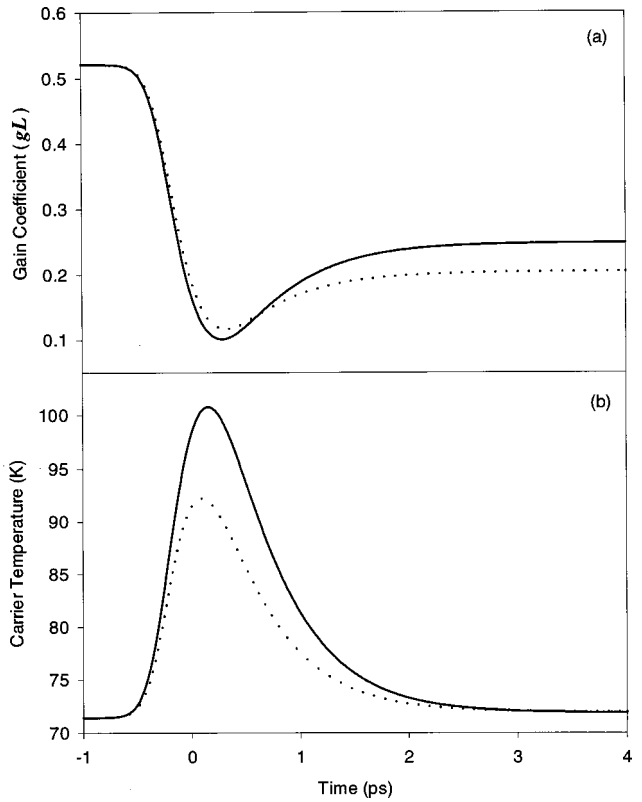

Fig. 5. Behavior of (a) the dimensionless gain coefficient and of (b) the carrier temperature, influenced by a 1-pJ pulse with FCA and TPA (solid curve), and without both (dotted curve) in an initially amplifying ($g > 0$) medium.

of FCA and TPA on the gain behavior is negligible, although their effect on the carrier temperature behavior is more apparent.

For an initially transparent medium (Figs. 3 and 4), the picture is quite different from that of an initially absorbing medium. Because the gain function is nearly zero, the only processes that can initially take place are FCA and TPA. The FCA makes states available at the band edge, and carrier–carrier scattering then leads to the establishment of a quasi-equilibrium ensemble with a higher temperature, i.e., fewer lower-energy levels and additional higher-energy levels are occupied. The TPA creates more carriers in the conduction band, but this process does not lead to an immediate increase in the gain function. This seemingly strange result has a simple explanation: The TPA creates hot carriers, which increases the average carrier temperature and thus leads to a lower value of the gain function (more absorption). The net result of these processes is an enhanced interband absorption, as is evident in Figs. 3(a) and 4(a). Consequently, we observe a change in carrier density from $\sim 1.671 \times 10^{18}\,\mathrm{cm}^{-3}$ to $\sim 1.672 \times 10^{18}\,\mathrm{cm}^{-3}$ for the 0.1-pJ pulse and to $\sim 1.708 \times 10^{18}\,\mathrm{cm}^{-3}$ for the 1.0-pJ pulse. In Figs. 3(b) and 4(b), we can see that the higher-energy pulse produces a larger maximum deviation of the carrier temperature from the lattice temperature; the ratio of the maximum temperature deviations (~ 9) is slightly less than the pulse energy ratio (10). These results also indicate that a substantial part of the carrier heating in the transparent medium is due to FCA. The influence of TPA in this case is much smaller as compared with FCA; for the 0.1-pJ pulse (Fig. 3), TPA is almost negligible.

The results for an initially amplifying medium show gain suppression accompanied by carrier heating (Fig. 5). For both 0.1 and 1.0-pJ pulse energies, we obtain qualitatively similar behavior, and Fig. 5 demonstrates the results only for the 1.0-pJ pulse. The carrier density decreases from $\sim 2.67 \times 10^{18}\,\mathrm{cm}^{-3}$ to $\sim 2.48 \times 10^{18}\,\mathrm{cm}^{-3}$ and to $\sim 2.04 \times 10^{18}\,\mathrm{cm}^{-3}$ for the 0.1- and 1.0-pJ pulses, respectively. In this case the influence of FCA and TPA is more noticeable; however, most of the carrier heating is due to interband transitions. Interband transitions here cause carrier heating because the carriers participating in these transitions are predominantly cold carriers. Thus the temperature of the carriers increases even though the total energy of the electronic ensemble decreases.

Next we apply pulses with energies $\mathscr{E}_x = 5.0$, 25.0 pJ; the results are presented in Figs. 6–10 below. All the other parameters used in these calculations are the same as those used to obtain Figs. 2–5. Results for the transparent medium in this case are omitted because no remarkable differences from the results for low-energy pulses were observed; the behavior is qualitatively the same. In Figs. 6 and 7 we can see both quantitative and qualitative changes in the dynamic behavior of the gain and carrier temperature from that presented in Fig. 2. Here the pulse energies are high enough to make the initially absorbing medium amplifying, and vice versa. For

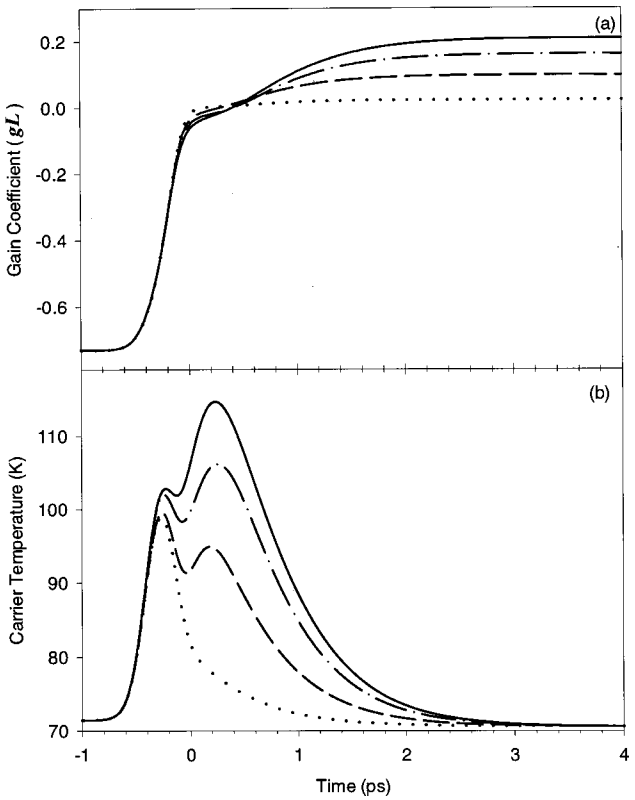

Fig. 6. Behavior of (a) the dimensionless gain coefficient and of (b) the carrier temperature, influenced by a 5-pJ pulse with FCA and TPA (solid curve), without FCA (dashed curve), without TPA (dashed–dotted curve), and without both (dotted curve) in an initially absorbing ($g < 0$) medium.

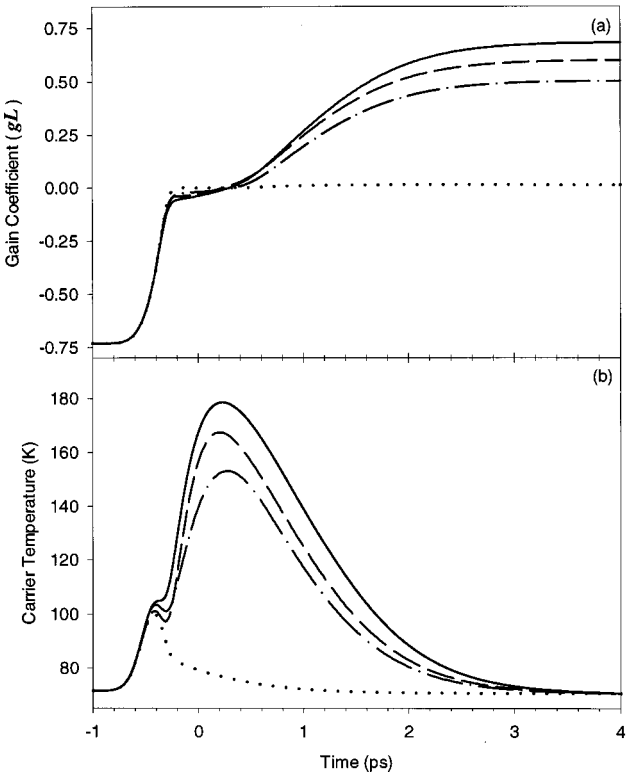

Fig. 7. Behavior of (a) the dimensionless gain coefficient and of (b) the carrier temperature, influenced by a 25-pJ pulse with FCA and TPA (solid curve), without FCA (dashed curve), without TPA (dashed–dotted curve), and without both (dotted curve) in an initially absorbing ($g < 0$) medium.

the absorbing medium (Figs. 6 and 7), the gain first reaches a plateau near the transparency region before becoming amplifying. For the amplifying medium (Figs. 8 and 9), we can see the usual gain suppression; however, while the 5.0-pJ pulse is amplified, the 25-pJ pulse actually experiences absorption [as is evident from the change in the carrier density before and after the pulse (see Fig. 10 and the numbers given immediately below)]. This is explained by the fact that the 25-pJ pulse saturates the gain faster than the 5.0-pJ pulse and by the fact that a substantial part of the 25-pJ pulse interacts with an absorbing medium rather than an amplifying medium. The carrier densities change from $\sim 2.67 \times 10^{18}\,\mathrm{cm}^{-3}$ to $\sim 2.1 \times 10^{18}\,\mathrm{cm}^{-3}$ for the 5-pJ pulse and to $\sim 3.59 \times 10^{18}\,\mathrm{cm}^{-3}$ for the 25-pJ pulse. FCA and TPA are both playing significant roles in the gain and carrier temperature dynamics. Whereas FCA has more influence for the 5-pJ pulse, TPA is dominating for the 25-pJ pulse. This is consistent with the fact that, whereas TPA is a quadratic function of the photon density, FCA is a linear function of the photon density.

The most unexpected behavior observed for higher pulse energies is the double-peak behavior of the carrier temperature for the absorbing medium of Figs. 6(b) and 7(b). The carrier cooling and reheating is different from the single-peak temperature behavior observed when lower external pulse energies are applied [Figs. 2(b)–5(b)], i.e. the temperature behavior changes qualitatively when the applied pulse has energy enough to bleach the sample. A second temperature peak appears, and its amplitude increases with increasing pulse energy. To our knowledge, this is the first report on this type of behavior of carrier temperature, so we shall discuss it in more detail. In particular, we are interested in the processes that lead to this type of behavior.

As we can see from the results described above, the carrier temperature increases owing to the energy influx that occurs through interband absorption, FCA, and TPA. Also, the carrier temperature can be affected by a change in the carrier density. More carriers also mean less energy per particle, and the temperature, as a measure of average energy, may decrease. While interband absorption brings energy to the system, it also increases the carrier density. This may decrease the temperature even though the total carrier energy is increased. FCA does not change the carrier density, but it increases the total energy of the system; thus it is always a heating factor. TPA changes the carrier density, but it creates only hot carriers. Although radiation takes energy away from the carrier ensemble, it also takes away cold carriers, thus leading to higher temperatures.

To understand the source of the second peak in the temperature response shown in Figs. 6(b) and 7(b), we should identify those processes that are significantly different in this case as compared with cases that show a single temperature peak. The second peak appears only in the case of an absorbing medium far from transparency when the pulse energy is high enough to bleach the me-

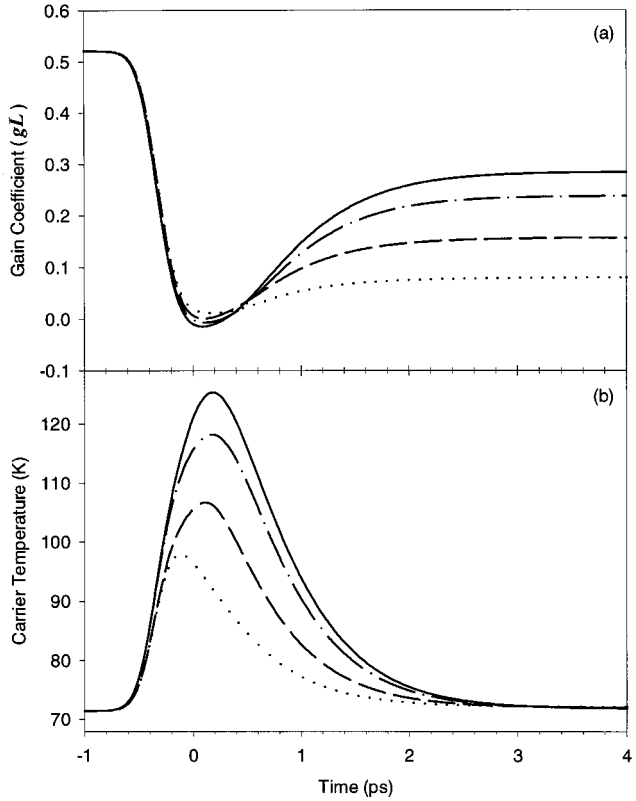

Fig. 8. Behavior of (a) the dimensionless gain coefficient and of (b) the carrier temperature, influenced by a 5-pJ pulse with FCA and TPA (solid curve), without FCA (dashed curve), without TPA (dashed–dotted curve), and without both (dotted curve) in an initially amplifying ($g > 0$) medium.

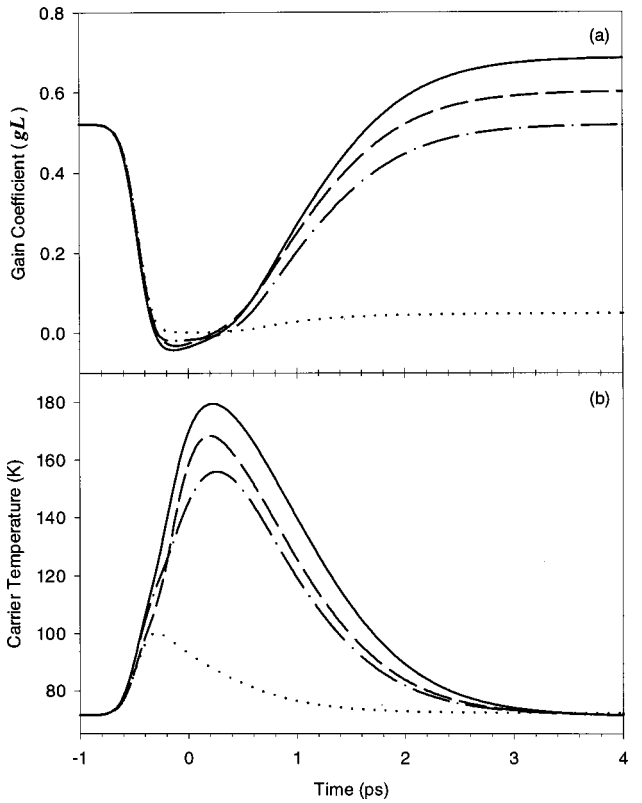

Fig. 9. Behavior of (a) the dimensionless gain coefficient and of (b) the carrier temperature, influenced by a 25-pJ pulse with FCA and TPA (solid curve), without FCA (dashed curve), without TPA (dashed–dotted curve) and without both (dotted curve) in an initially amplifying ($g > 0$) medium.

dium; hence we are dealing with substantial changes in both carrier and photon densities. FCA is proportional to both carrier and photon densities, and, therefore, in this case the efficiency of FCA is much higher than in the other cases. TPA also experiences significant growth in efficiency, since it is proportional to the square of the photon density. So we expect both FCA and TPA to be responsible for the double-peak behavior. This thesis is supported by the results obtained when both FCA and TPA are eliminated artificially from the numerical experiment setting $s_{\mathrm{FCA}} = s_{\mathrm{TPA}} = 0$. As can be seen, interband transitions dominate the early dynamics but become less important after the gain reaches the plateau near the transparency region [see Figs. 6(a) and 7(a)]. At this point the cooling effect due to the increased number of carriers overcomes the heating effect due to the energy influx, and we see a decrease in temperature. When the medium becomes transparent and the interband absorption stops, the carrier temperature relaxes owing to interaction with the lattice (phonon emission). Note that, without both FCA and TPA, the gain function remains close to the transparency region (dotted curves in Figs. 6 and 7), although carrier cooling leads to a slight increase in the gain function afterward. However, when either FCA or TPA is present (dotted–dashed or dashed curves in Figs. 6 and 7), the second peak appears in the temperature graphs. Furthermore, the first peak appears in the absorption region when the pulse is partially absorbed and the dominant heating factor is the (single-photon) absorption (note the small difference at the first peak between the curves showing the cases with and without FCA and TPA). The second peak appears when the pulse is completely absorbed and when the medium is in the transparency region where the FCA and TPA are the dominant heating mechanisms. As in the case of the amplifying sample, for the 5-pJ pulse, FCA is dominant; for the 25-pJ pulse, TPA has more influence. Finally, the medium becomes amplifying when the carriers cool down. With FCA and TPA the medium absorbs more, increasing carrier density. The FCA does not change the carrier density by itself; however, it assists the single-photon absorption by making electronic states available at the bottom of the energy band.

Another observation that we would like to point out is the noncumulative influence of FCA and TPA. The maximum carrier temperature change that is due to the total heating effect of FCA and TPA is less than the sum of the changes obtained when only FCA or TPA is included. They both are independent heating factors; however, they heat the carrier ensemble more efficiently when they act separately. This is especially evident for high-energy pulses when FCA and TPA have quantitatively similar effects. Both FCA and TPA create carriers in the same region of the energy levels in the conduction band—approximately $\hbar\omega$ above the band edge. Having more carriers in this region leads to lower probabilities of transitions from the band edge (FCA) and from the valence

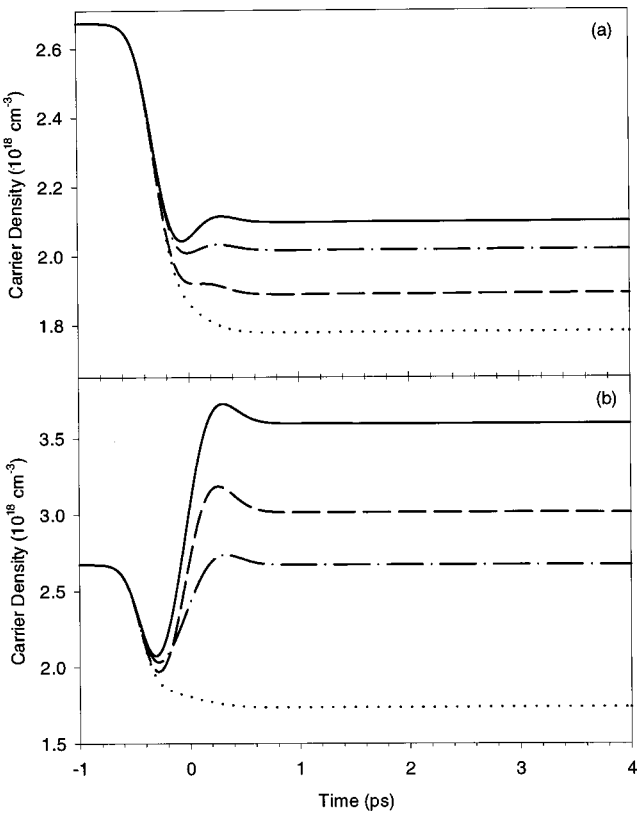

Fig. 10. Behavior of the carrier density influenced by (a) 5-pJ and (b) 25-pJ pulses with FCA and TPA (solid curve), without FCA (dashed curve), without TPA (dashed–dotted curve), and without both (dotted curve) in an initially amplifying ($g > 0$) medium.

band (TPA). Thus in this context FCA and TPA are self- and mutually saturating processes.

Finally, we note that, although the bandgap energy is a function of carrier density that is due to many-body effects [see Eq. (20)], this dependence does not noticeably affect the dynamic behavior of the gain and the carrier temperature for pulse energies considered in this study. Higher pulse energies and, hence, more dramatic changes in the carrier density are expected to have a more visible influence on dynamic variables.

5. SUMMARY

Using a model that is based on modified rate equations, we have considered the dynamic behavior of the gain and carrier temperature in a short semiconductor medium subject to external optical pulses on a picosecond time scale. Our model gives a simple description of the dynamics and allows for a clear physical interpretation. The rate equations for photon and carrier densities are modified to include a third rate equation for the energy density and to allow for the use of an analytical approximation for the complex dependence of the gain on the chemical potential and temperature of the carriers. The model relies on the assumption of a quasi-equilibrium Fermi–Dirac carrier distribution and, therefore, all of the dynamic behavior is a result of the interactions of the quasi-equilibrium carrier ensemble with the external pulse and the lattice. We are effectively treating the carrier temperature as a dynamic variable. Nonequilibrium processes such as spectral hole burning are not present in this model; their effect becomes significant on the femtosecond time scale.[19]

We study the cases for media whose prepulse states are strongly absorbing, transparent, and strongly amplifying at the frequency of the pulse. The results show that the various physical processes that influence the gain and the carrier temperature contribute differently, depending on both the initial state of the medium and the pulse energy. In particular, we note the competing effects associated with the pulse's changing the energy density and the carrier density simultaneously. We also point out how FCA and TPA can dominate when the gain is near the transparency region. This domination leads to an initial gain suppression followed by gain enhancement that is due to interband absorption made possible by FCA and TPA, as shown in Fig. 5. It can also lead to a double peak in the carrier temperature response and a plateau followed by an increase in the gain, as shown and explained in Figs. 6 and 7, where the contributions of FCA and TPA are made explicit. Although FCA and TPA are both heating factors, their influence is noncumulative.

The results presented in this paper can be verified with existing experimental techniques.[41] Additional controllable signals can be used to provide more-accurate information about the gain and carrier temperature dynamics.

ACKNOWLEDGMENTS

This work is partially supported by National Science Foundation grant ECS-9215852 and by Russian Foundation for Basic Research grant 96-02-16690.

D. K. Bandy can be reached by e-mail at bandy@hollywood.laserctr.okstate.edu.

REFERENCES

1. M. S. Stix, M. P. Kesler, and E. P. Ippen, "Observations of subpicosecond dynamics in GaAlAs laser diodes," Appl. Phys. Lett. **48**, 1722–1725 (1986).
2. W. Z. Lin, L. G. Fujimoto, E. P. Ippen, and R. A. Logan, "Femtosecond carrier dynamics in GaAs," Appl. Phys. Lett. **50**, 124–126 (1987).
3. M. P. Kesler and E. P. Ippen, "Subpicosecond gain dynamics in GaAlAs laser diodes," Appl. Phys. Lett. **51**, 1765–1767 (1987).
4. K. L. Hall, J. Mark, E. P. Ippen, and G. Eisenstein, "Femtosecond gain dynamics in InGaAsP optical amplifiers," Appl. Phys. Lett. **56**, 1740–1742 (1990).
5. J. Mark and J. Mørk, "Subpicosecond gain dynamics in InGaAsP optical amplifiers: experiment and theory," Appl. Phys. Lett. **61**, 2281–2283 (1992).
6. B. N. Gomatam and A. P. DeFonzo, "Theory of hot carrier effects on non-linear gain in GaAs–GaAlAs lasers and amplifiers," IEEE J. Quantum Electron. **26**, 1689–1704 (1990).
7. M. Willatzen, A. Uskov, J. Mørk, H. Olesen, B. Tromborg, and A.-P. Jauho, "Nonlinear gain suppression in semiconductor lasers due to carrier heating," IEEE Photon. Technol. Lett. **3**, 606–609 (1991).
8. A. N. Oraevsky, M. M. Clark, and D. K. Bandy, "Many-temperature model of laser with dynamics," Opt. Commun. **85**, 360–364 (1991).
9. M. Willatzen, T. Takahashi, and Y. Arakawa, "Nonlinear gain effects due to carrier heating and spectral hole burning in strained-quantum well lasers," IEEE Photon. Technol. Lett. **4**, 682–685 (1992).
10. A. V. Uskov, J. Mørk, and J. Mark, "Theory of short-pulse gain saturation in semiconductor laser amplifiers," IEEE Photon. Technol. Lett. **4**, 443–446 (1992).
11. V. I. Tolstikhin and M. Willander, "Carrier heating effects in dynamic-single-frequency GaInAsP–InP laser diodes," IEEE J. Quantum Electron. **31**, 814–833 (1995).
12. C. Z. Ning, R. A. Indik, and J. V. Moloney, "Self-consistent approach to thermal effects in vertical-cavity surface-emitting lasers," J. Opt. Soc. Am. B **12**, 1993–2004 (1995).
13. C.-Y. Tsai, R. M. Spencer, Y.-H. Lo, and L. F. Eastman, "Nonlinear gain coefficients in semiconductor lasers: effects of carrier heating," IEEE J. Quantum Electron. **32**, 201–212 (1996).
14. R. A. Indik, R. Binder, M. Mlejnek, J. V. Moloney, S. Hughes, A. Knorr, and S. W. Koch, "Role of plasma cooling, heating, and memory effects in subpicosecond pulse propagation in semiconductor amplifiers," Phys. Rev. A **53**, 3614–3620 (1996).
15. A. N. Oraevsky, T. V. Sarkisyan, and D. K. Bandy, "Nonlinear gain and bistable regime of free-running oscillation in a semiconductor laser," Laser Phys. **7**, 920–927 (1997).
16. T. V. Sarkisyan, A. N. Oraevsky, A. T. Rosenberger, R. L. Rolleigh, and D. K. Bandy, "Nonlinear gain and carrier temperature dynamics in semiconductor laser media," J. Opt. Soc. Am. B **15**, 1107–1119 (1998).
17. V. M. Galitskii and V. F. Elesin, *Resonant Interaction of Electromagnetic Fields with Semiconductors* (Energoatomizdat, Moscow, 1986) (in Russian).
18. W. Schäfer and K. Henneberger, "Pulse propagation and carrier kinetics in laser excited semiconductors," Phys. Status Solidi B **159**, 59–69 (1990).
19. A. Knorr, R. Binder, M. Lindberg, and S. W. Koch, "Theoretical study of resonant ultrashort-pulse propagation in semiconductors," Phys. Rev. A **46**, 7179–7186 (1992).
20. H. Haug and S. W. Koch, *Quantum Theory of the Optical and Electronic Properties of Semiconductors* (World Scientific, Singapore, 1993).
21. C. M. Bowden and G. P. Agrawal, "Bloch–Maxwell formulation for semiconductors: effects of coherent Coulomb exchange," Phys. Rev. A **51**, 4132–4139 (1995).

22. O. Hess and T. Kuhn, "Maxwell–Bloch equations for spatially inhomogeneous semiconductor lasers. I. Theoretical formulation," Phys. Rev. A **54**, 3347–3359 (1996).
23. G. H. B. Thompson, *Physics of Semiconductor Laser Devices* (Wiley, New York, 1980).
24. G. P. Agrawal and N. K. Dutta, *Semiconductor Lasers* (Van Nostrand Reinhold, New York, 1993).
25. L. A. Coldren and S. W. Corzine, *Diode Lasers and Photonic Integrated Circuits* (Wiley, New York, 1995).
26. S. L. Chuang, *Physics of Optoelectronic Devices* (Wiley, New York, 1995), p. 358.
27. L. A. Rivlin, A. T. Semenov, and S. D. Yakubovich, *Dinamika i Spektry Izlucheniya Poluprovodnikovykh Lazerov* (Radio Svyaz, Moscow, 1983) (in Russian).
28. L. A. Rivlin, "Dynamics and emission spectra of semiconductor lasers," J. Sov. Laser Res. **7**, 57–206 (1986).
29. *Semiconductors: Group IV Elements and III–V Compounds*, O. Madelung, ed. (Springer-Verlag, Berlin, 1991), pp. 101–113.
30. J. Mørk and A. Mecozzi, "Theory of the ultrafast optical response of active semiconductor waveguides," J. Opt. Soc. Am. B **13**, 1803–1816 (1996).
31. H. C. Casey, Jr., and F. Stern, "Concentration-dependent absorption and spontaneous emission in heavily doped GaAs," J. Appl. Phys. **47**, 631–643 (1976).
32. H. C. Casey, Jr., and M. B. Panish, *Heterostructure Part B: Materials and Operating Characteristics* (Academic, New York, 1978).
33. M. Sheik-Bahae, D. C. Hutchings, D. J. Hagan, and E. W. Van Stryland, "Dispersion of bound electronic nonlinear refraction in solids," IEEE J. Quantum Electron. **27**, 1296–1309 (1991).
34. A. Villeneuve, M. Sundheimer, N. Finalayson, G. I. Stegeman, S. Morasca, C. Rigo, R. Calvani, and C. DeBernardi, "Two-photon absorption in $In_{1-x-y}Ga_xAl_yAs/InP$ waveguides at communications wavelengths," Appl. Phys. Lett. **56**, 1865–1867 (1990).
35. J. R. Karin, A. V. Uskov, R. Nagarajan, J. E. Bowers, and J. Mørk, "Carrier heating dynamics in semiconductor waveguide saturable absorbers," Appl. Phys. Lett. **65**, 2708–2711 (1994).
36. A. V. Uskov, J. R. Karin, R. Nagarajan, and J. E. Bowers, "Dynamics of carrier heating and sweepout in waveguide saturable absorbers," IEEE J. Sel. Top. Quantum Electron. **1**, 552–561 (1995).
37. A. V. Uskov, J. R. Karin, J. E. Bowers, J. G. McInerney, and J. Le Bihan, "Effects of carrier cooling and carrier heating in saturation dynamics and pulse propagation through bulk semiconductor absorbers," IEEE J. Quantum Electron. **34**, 2162–2171 (1998).
38. D. Bimberg and J. Mycielski, "Recombination-induced heating of free carriers in a semiconductor," Phys. Rev. B **31**, 5490–5493 (1985).
39. D. Bimberg and J. Mycielski, "The recombination-induced temperature change of no-equilibrium charge carriers," J. Phys. C **19**, 2363–2373 (1986).
40. A. N. Oraevsky, T. Sarkisyan, and D. K. Bandy, "Dynamics of the temperature of a recombining ensemble of fermions," JETP Lett. **62**, 673–676 (1995).
41. P. Borri, S. Scaffetti, J. Mørk, W. Langbein, J. M. Hvam, A. Mecozzi, and F. Martelli, "Measurement and calculation of the critical pulsewidth for gain saturation in semiconductor optical amplifiers," Opt. Commun. **164**, 51–55 (1999).